Applied Catalysis B: Environmental 202 (2017) 695–703

Contents lists available at ScienceDirect

Applied Catalysis B: Environmental

journal homepage: www.elsevier.com/locate/apcatb

Selective photocatalytic reduction of CO_2 into CH_4 over Pt-Cu_2O TiO_2 nanocrystals: The interaction between Pt and Cu_2O cocatalysts

Zhuo Xiong[a], Ze Lei[a], Chia-Chien Kuang[b], Xiaoxiang Chen[a], Bengen Gong[a], Yongchun Zhao[a,*], Junying Zhang[a,*], Chuguang Zheng[a], Jeffrey C.S. Wu[b]

[a] State Key Laboratory of Coal Combustion, School of Energy and Power Engineering, Huazhong University of Science & Technology, 1037 Luoyu Road, Wuhan 430074, China
[b] Department of Chemical Engineering, National Taiwan University, No. 1, Section 4, Roosevelt Road, Taipei 10617, Taiwan

ARTICLE INFO

Article history:
Received 22 July 2016
Received in revised form
22 September 2016
Accepted 3 October 2016
Available online 4 October 2016

Keywords:
CO_2 photocatalytic reduction
Selectivity
Cocatalyst
Interaction

ABSTRACT

Photocatalytic reduction of CO_2 with water is one of the most popular and challenging technologies to produce renewable energy. In this paper, Pt and Cu_2O nanoparticles (NPs) were deposited on the surface of anatase TiO_2 nanocrystals, and their effects on the photocatalytic performance of TiO_2 were thoroughly studied. Based on experimental results, Pt tended to promote the production of CH_4 and H_2. However, Cu_2O suppressed H_2 production and exhibited lower CH_4 selectivity than that of Pt. Furthermore, when Pt and Cu_2O were co-deposited on TiO_2 crystals, H_2 production was inhibited and CO_2 was selectively converted into CH_4. From characterization, we found that Pt could not only capture photogenerated electrons and but also increase the electrons density on the catalyst, which were beneficial for selective CH_4 formation. In addition, co-deposited Cu_2O enhanced the CO_2 chemisorption on TiO_2 while inhibited that of water, resulting in enhancement of CO_2 reduction and lower H_2 production. On account of the above-mentioned contribution of Pt and Cu_2O NPs, Pt-Cu_2O/TiO_2 catalyst showed high CH_4 selectivity towards all products from reductive reaction.

1. Introduction

CO_2 has been recognized as the main greenhouse gas contributing to global warming. Therefore, one of the best solutions to this issue is to convert CO_2 into renewable fuels by utilizing solar energy, which not only can reduce CO_2 emission but also provide useful energy sources [1–3]. Since Inoue et al. [4] first reported the CO_2 photocatalytic reduction over semiconductor materials in 1979, TiO_2 has become a favored photocatalyst because of its availability, stability, low cost, and low toxicity [5,6]. However, due to fast recombination of photogenerated electron-hole pairs and limited utilization of solar energy, TiO_2 shows low photocatalytic reaction efficiency [7]. In addition, the weak adsorption and interaction of CO_2 on TiO_2 surface also limit the efficiency of CO_2 photocatalytic reduction.

Many strategies, including preparing TiO_2 with different structures or morphologies [8–10], decorating TiO_2 with noble metals [11–14], and combining TiO_2 with other materials [15,16] have been reported as routes to enhance the efficiency of CO_2 photocatalytic reduction. In our previous work [17], we reported that TiO_2 nanocrystals with co-exposed {101} and {001} facets exhibited enhanced CO_2 photocatalytic reduction activity, which resulted from promoted spatial separation of photogenerated charges towards the different facets of TiO_2 nanocrystals. However, most of these strategies promote H_2 production from water splitting as well, which is completive with CO_2 photocatalytic reduction. Besides, it is still difficult to selectively convert CO_2 into the specific product. Recently, Xie et al. [18] reported that Pt-MgO/TiO_2 enhanced the selectivity of CH_4 production from CO_2 photoreduction because MgO enhanced CO_2 chemsorption and Pt increased electron density. Zhai et al. [19] prepared Pt@Cu_2O core-shell structured cocatalyst and found it enhanced CO_2 reduction while suppressed the reduction of water to H_2. Many studies have reported that cocatalysts are able to enhance photocatalytic efficiency of TiO_2, however, still limited researches have discussed the effects of cocatalysts contributed to the product selectivity in CO_2 reduction.

In this paper, anatase TiO_2 nanocrystals with co-exposed {101} and {001} facets were prepared through a solvothermal method. After that, Pt and Cu_2O NPs were deposited on the surface of TiO_2 crystals as cocatalysts. The effects of cocatalysts on the photocat-

* Corresponding authors.
E-mail addresses: yczhao@hust.edu.cn (Y. Zhao), jyzhang@hust.edu.cn (J. Zhang).

http://dx.doi.org/10.1016/j.apcatb.2016.10.001
0926-3373/

alytic activity of TiO_2 and product selectivity were investigated. Finally, a possible reaction mechanism about the selectivity of the catalysts was proposed based on experimental results. This study attempts to provide a new insight for the design of photocatalysts with high selectivity for CO_2 reduction.

2. Experimental

2.1. Catalyst preparation

2.1.1. Preparation of TiO_2 nanocrystals

TiO_2 nanocrystals with co-exposed {001} and {101} facets were prepared by a solvothermal method reported in our previous work [17]. First, 10 mL titanium butoxide and 1.2 mL HF solution were added into 90 mL ethanol under sonication for 1 h. The mixed solution was transferred into a 200 mL Teflon-lined autoclave and kept at 180 °C for 24 h. Later, the autoclave was cooled naturally to ambient temperature. The white precipitate in the clave was collected by centrifugation, washed with ethanol and deionized water for 3 times, and then dried in an oven at 60 °C for 12 h. To remove fluorine residues, the TiO_2 powder was further calcined in air atmosphere (500 °C, 2 h).

2.1.2. Deposition of Pt and Cu_2O NPs onto TiO_2 nanocrystals

Pt and Cu_2O NPs were co-deposited onto TiO_2 nanocrystals by using a chemical reduction method with the help of $NaBH_4$. In a typical process, 1 g TiO_2 nanocrystal powders were dispersed in a 50 mL H_2PtCl_6 and $Cu(CH_3COO)_2$ mixed aqueous solution under stirring for 30 min. The mass ratio of Pt or Cu to TiO_2 is 1%. Then 5 mL of mixed solution of $NaBH_4$ solution (0.1 M) and NaOH solution (0.5 M) were added into the TiO_2 suspension under vigorous stirring for 30 min. After reduction, the solid samples were washed with DI water and collected by centrifugation and drying at 60 °C overnight. The obtained sample was donated as Pt-Cu_2O/TiO_2. Besides, Pt/TiO_2 and Cu_2O/TiO_2 were fabricated by dispersing TiO_2 into the metal precursor solution (*only* H_2PtCl_6 *or* $Cu(CH_3COO)_2$), which is similar to the above-mentioned method.

2.2. Catalyst characterization

For all samples, X-ray diffraction (XRD) patterns were recorded on an Empyrean diffractometer using Cu Kα radiation (λ = 0.1542 nm) in the range of 10–80°. The specific surface areas and pore size distribution were measured by a Micrometrics ASAP 2020 surface area and porosity analyzer. Transmission electron microscopy (TEM) images were obtained using an FEI Tecnai G^2 F30 instrument. X-ray photoelectron spectra (XPS) were recorded on a Shimadzu/KRATOS AXIS-ULTRA DLD-600W instrument equipped with Al/Mg Kα radiation. Photoluminescence spectra (PL) were recorded on a confocal laser Raman microscope (Horiba JobinYvon, LabRAM HR800) using a 325 nm excitation light source.

In order to verify the behavior of the catalysts in the presence of CO_2, all samples were analyzed by temperature programmed CO_2 desorption (TPD-CO_2). This technique enables us to analyze the types of sites existing in the materials. For the procedures in detail, 50 mg sample of powder was placed into a quartz tube reactor first, which was heated under ultra-high purity He flow (30 mL min^{-1}) up to 300 °C at a rate of 25 °C min^{-1} for 1 h and then cooled to ambient temperature. After the pretreatment, CO_2 flow (30 mL min^{-1}) passed through the catalyst bed for 30 min, subsequently the sample was flushed by He flow (30 mL min^{-1}) for 1 h. Finally, the TPD analysis was performed under He flow (30 mL min^{-1}) by heating the reactor up to 750 °C (Rate: 10 °C min^{-1}). The effluent gas flow was monitored by a TCD detector.

Table 1
Specific surface areas, pore volumes, and pore sizes of the catalysts.

Samples	BET surface area/m^2 g^{-1}	Pore volume/cm^3 g^{-1}	Pore size/nm
TiO_2	167.4	0.28	6.7
Cu_2O/TiO_2	165.0	0.30	7.2
Pt/TiO_2	165.6	0.29	6.9
$Pt\text{-}Cu_2O/TiO_2$	166.8	0.29	7.0

2.3. Photocatalytic reduction of CO_2

CO_2 photocatalytic reduction under UV light irradiation was carried out in an internal circulated reaction system (as shown in Fig. 1), including a 500 mL Pyrex glass reactor with a quartz window at the top, a 300 W Xe lamp positioned 10 cm above the reactor, and an online gas chromatography (GC). The UV light (300 nm < λ < 400 nm, 20.5 mW cm^{-2}) was obtained by using a UV light reflector. 10 mL of deionized water was added in the bottom of the reactor, and then 20 mg of catalyst powders was placed on a Petri plate positioned 2 cm above the water in the reactor. Prior to illumination, the reactor was first vacuumed by a pump and then was purged and filled by ultra pure CO_2 (99.999%). The internal pressure of the reactor was 71 kPa and the temperature of the reactor was kept at 20 °C by cooling it with circulating water. The vapor pressure of water was 2.3 kPa under this situation. During 4 h UV light irradiation, the amounts of H_2, CO, and hydrocarbons in the reactor were analyzed by a GC every 15 min. The GC was equipped with a flame ionization detector (FID), a thermal conductivity detector (TCD), and a methanizer. The gaseous sample containing H_2, O_2, N_2, CO, CO_2, and hydrocarbons flowed through a carbon molecular sieve column (TDX-01) to flush CO_2 back to the atmosphere. After that, H_2, O_2, N_2, CO, and hydrocarbons in the sample were separated by a molecular sieve 5A column. Finally, H_2, O_2, and N_2 in the sample were analyzed by the TCD, while CH_4 and CO (converted to CH_4 by a methanizer) were analyzed by the FID. Ar was the carrier gas of GC.

Several blank experiments were performed to ensure that any carbon-containing products measured by GC indeed originated from purged CO_2. First, tests using CO_2 and water as reactants were conducted in the empty reactor. No hydrocarbons were detected in the dark or under light irradiation in this case. This indicated that the CO_2 reduction reaction could not happen in the absence of catalyst. Also, when the reactor was vacuumed (without purged CO_2), no hydrocarbons were detected under UV light irradiation in the presence of water and catalyst.

3. Results and discussion

3.1. Characterization of the catalysts

Fig. 2 shows the XRD patterns of as-prepared samples. Among all the samples, TiO_2 was in anatase form and no diffraction peaks for Pt or Cu species were observed, which may result from the low loaded content or fine dispersion of metal species on the surface of TiO_2 crystals [8,20]. The patterns showed that the deposition of metal species did not affect the crystal structure of anatase TiO_2.

N_2 adsorption-desorption was used to explore the textual properties of the catalysts. The BET surface area, pore volume, and pore size of the samples were summarized in Table 1. The BET surface areas of the all samples are nearly identical (*ca.* 165 m^2 g^{-1}). The loaded metal species barely affect the surface areas, pore size, and pore structure of TiO_2 nanocrystals.

The TEM and HR-TEM images of the samples are shown in Fig. 3. The pure TiO_2 nanocrystal is a truncated tetragonal bipyramidal enclosed by eight {101} facets on sides and two {001} facets on the top and bottom (Fig. 3A). The side length and thickness of TiO_2

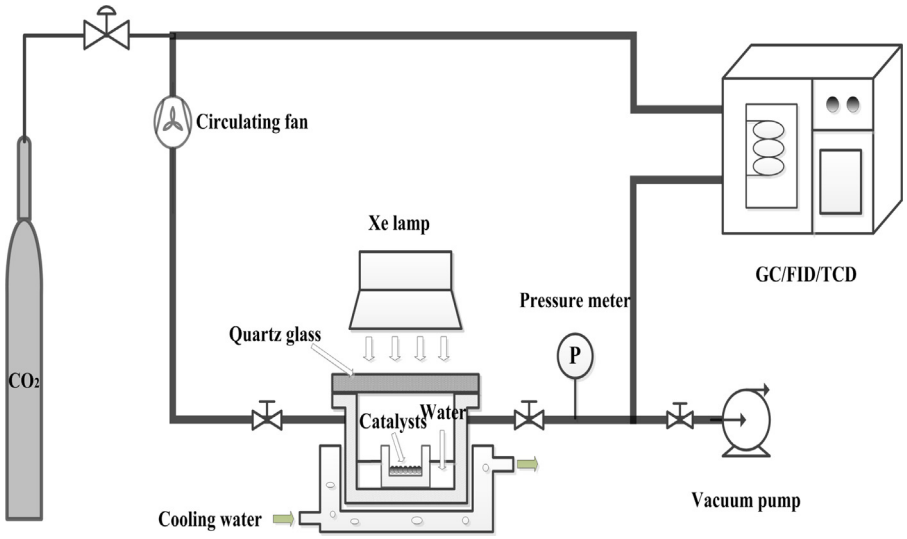

Fig. 1. Schematic of experimental setup for CO_2 photocatalytic reduction.

nanocrystal was approximately 50 nm and 20 nm. The ratio of the {001} facets was calculated to be around 40% based on the method reported in the literature [21]. Fig. 3B–C shows the TEM and HR-TEM of Pt/TiO_2 sample. Many small black spots were observed on the surface of TiO_2 NPs. According to the interplanar spacing in Fig. 3C, these black spots were identified as Pt particles [20,22]. The TEM images of Cu_2O/TiO_2 catalysts are shown in Fig. 3D–F. The TiO_2 nanocrystals with co-exposed {101} and {001} facets was clearly observed but Cu was difficult to be found in Fig. 3D, which may be caused by the small size and low crystallinity of Cu species. In Fig. 3E, with higher resolution, Cu species deposited on the surface can be clearly observed, which existed as Cu_2O according to the interplanar spacing shown in Fig. 3F [19]. For Pt-Cu_2O/TiO_2 catalyst (shown in Fig. 3G–H), both Pt and Cu_2O NPs could be distinguished on the surface of TiO_2 crystals.

XPS was used to investigate the chemical states of Pt, Cu, Ti, and O on the surface of the catalysts.

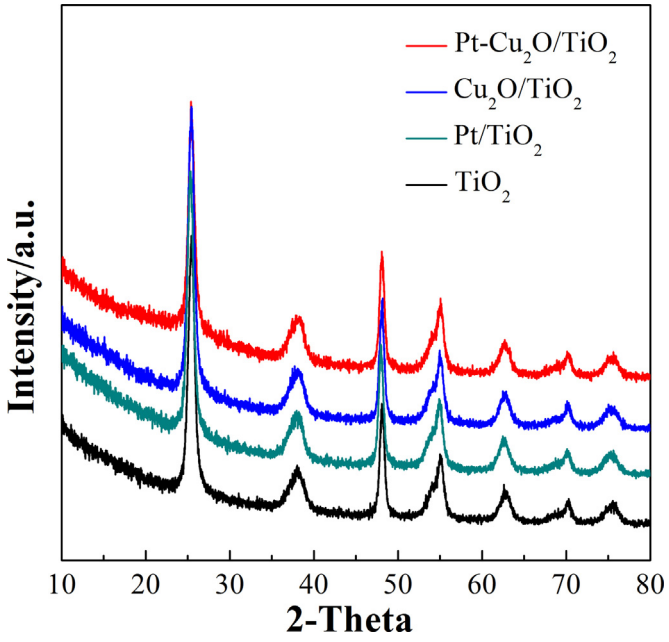

Fig. 2. XRD patterns of the as-prepared catalysts.

Fig. 4A shows the high-resolution Ti 2p XPS spectra of Pt/TiO_2. There exist two peaks in the binding energy region of Ti 2p. The binding energy of Ti $2p_{3/2}$ for each sample is around 458.6 eV, which indicates Ti^{4+} in the TiO_2 [23,24]. The high-resolution O 1 s XPS spectra of all the samples in Fig. 4B can be resolved into two peaks. The one with lower energy (around 530.0 eV) is assigned to oxygen in TiO_2 lattice (O_L) and the other (531.5 eV) can be ascribed to superficial oxygen of hydroxyl species (O_H) [17]. The O_H/O_L molar ratio of TiO_2, Pt/TiO_2, Cu_2O/TiO_2, and Pt-Cu_2O/TiO_2 were 0.203, 0.243, 0.269, and 0.338, respectively. This information suggests that both deposited Pt and Cu increased the amount of O_H on TiO_2, which may enhance of CO_2 adsorption and its catalytic activity [20,25,26]. The high-resolution Pt 4f XPS spectra of Pt/TiO_2 and Pt-Cu_2O/TiO_2 catalysts are shown in Fig. 4C. The Pt 4f region contains two peaks, which can be resolved into two pairs of XPS peaks. The peaks can be attributed to Pt^0 (70.6 eV, 74.1 eV) and Pt^{2+} (71.4 eV and 75.5 eV) [23,24]. The existence of Pt^{2+} might result from partial oxidation of Pt NPs [27]. Meanwhile, the binding energy of Pt 4 almost unchanged, showing the electron density on Pt was not influenced by co-deposited Cu_2O. Fig. 4D shows the high-resolution Cu 2p XPS spectra of Cu_2O/TiO_2 and Pt-Cu_2O/TiO_2 catalysts. The binding energy of Cu $2p_{3/2}$ for Cu_2O/TiO_2 was ca. 932.5 eV, indicating that the Cu species exist as Cu_2O [19,26]. This is in line with the results from TEM. Besides, compared to the peak position of Cu_2O/TiO_2 catalyst, it is notable that the Cu 2p peaks of Pt-Cu_2O/TiO_2 shows slight shift to lower binding energy, which implies that Pt promoted the electron migration towards Cu_2O NPs. The phenomenon also indicated increased electron density on Cu_2O NPs.

PL spectrum was useful for the investigation of electron-hole recombination in semiconductor, which induces fluorescence. The PL spectra of the catalysts are shown in Fig. 5. Their PL spectra were similar to each other except for different fluorescence intensity. Generally, fluorescence intensity declines in accordance of reduced photogenerated electron-hole recombination [28]. In our previous work [17], we found that the co-exposed {101} and {001} facets of TiO_2 nanocrystals promoted the separation of photogenerated charges because photogenerated electrons on the anatase TiO_2 nanocrystals prefer to migrate to the {101} facets while the photogenerated holes tend to transfer to the {001} facets [21,29]. In this work, the deposition of Pt and Cu_2O NPs on TiO_2 nanocrystals both suppressed the PL intensity of TiO_2 nanocrystals. This is because the Pt and Cu_2O NPs deposited on the {101} facets of TiO_2 crystals can easily capture the photogenerated electrons accumulated on

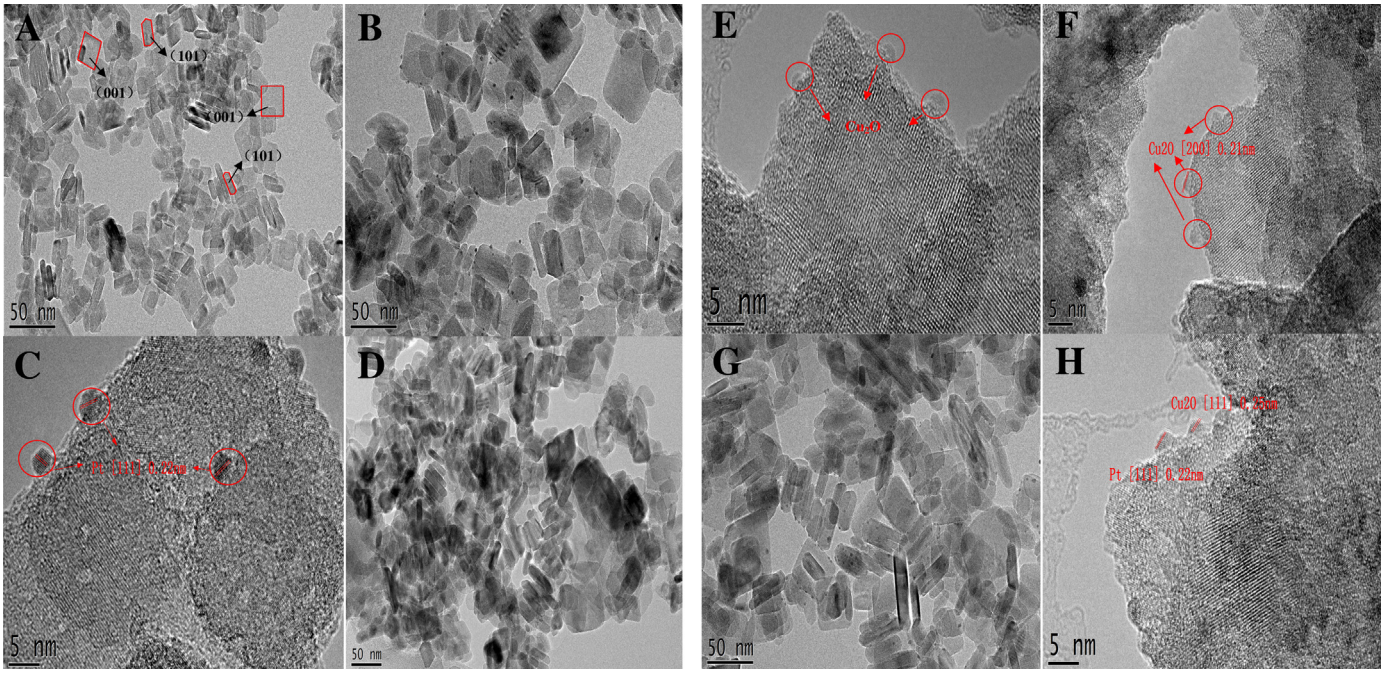

Fig. 3. TEM and HR-TEM images of TiO_2 (A), Pt/TiO_2 (B-C), Cu_2O/TiO_2 (D-F), and $Pt\text{-}Cu_2O/TiO_2$ (G-H) catalysts.

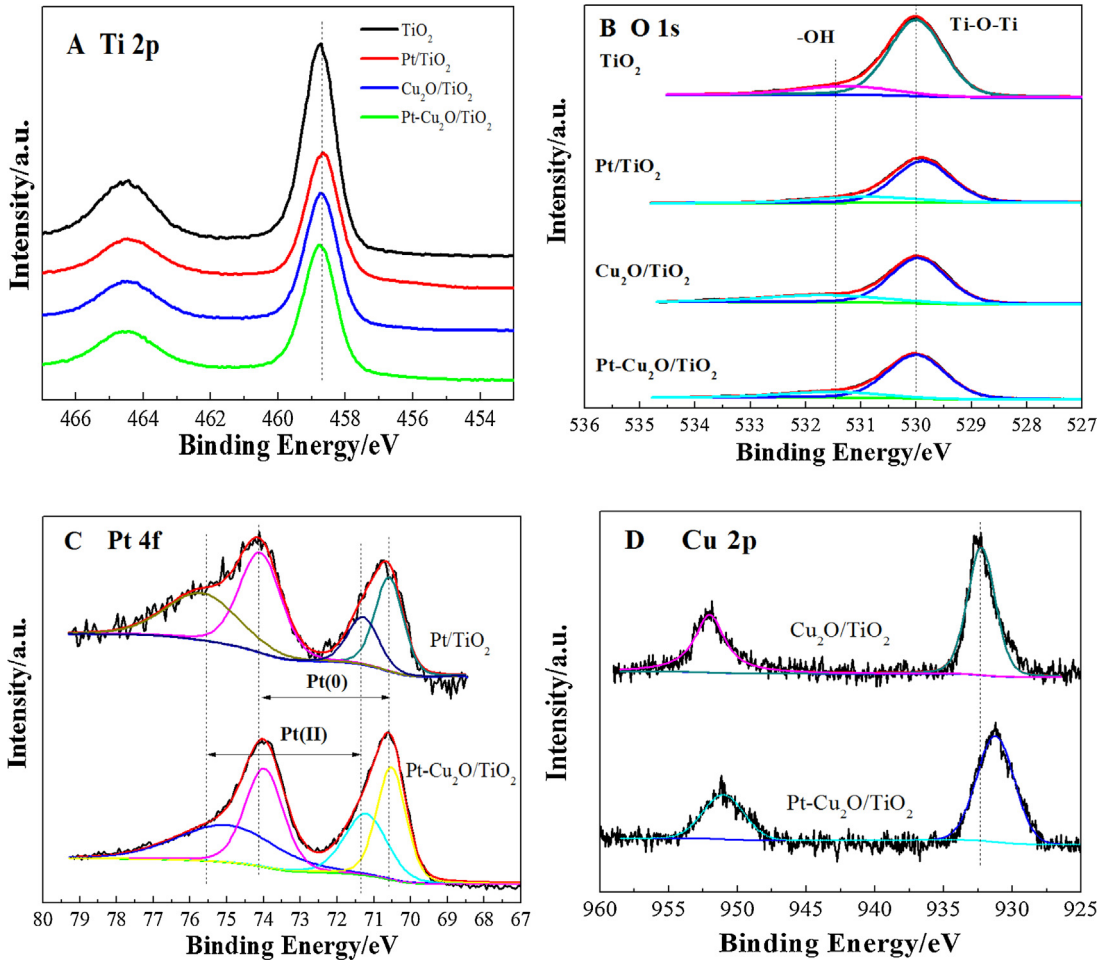

Fig. 4. XPS spectra of the as-prepared samples: (A) High-resolution Ti 2p spectra; (B) High-resolution O 1s spectra; (C) High-resolution Pt 4f spectra; (D) High-resolution Cu 2p spectra.

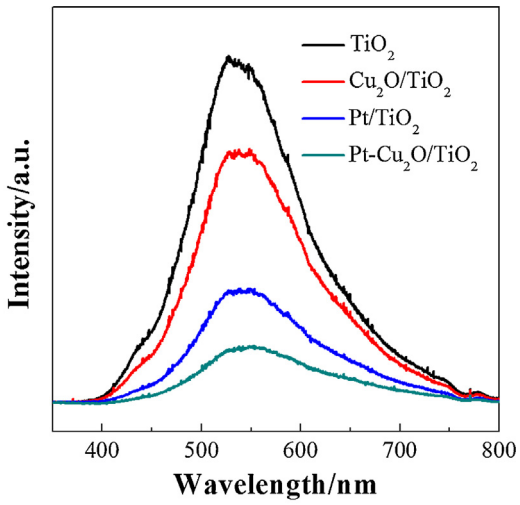

Fig. 5. The photoluminescence spectra of the catalysts.

Table 2
Photocatalytic activities and selectivities of as-prepared samples.

Samples	CO_2 chemisorbed /μmol g^{-1}	Yields/μmol g^{-1} h^{-1}				Selectivity/%		
		H_2	CO	CH_4	O_2	H_2	CO	CH_4
TiO_2	6.3	0.39	0.64	0.22	1.02	31.1	51.1	17.8
Pt/TiO_2	6.8	0.72	0.17	0.42	1.31	33.8	8.1	58.1
Cu_2O/TiO_2	10.6	0	0.42	0.99	2.22	0	29.9	70.1
$Pt\text{-}Cu_2O/TiO_2$	11.0	0	0.05	1.42	2.95	0	3.4	96.6

the {101} facets, promoting the spatial separation of photogenerated electrons and holes effectively. The PL intensity of Pt/TiO_2 was lower, indicating that Pt NPs inhibited the recombination of photogenerated charges more effectively than Cu NPs. $Pt\text{-}Cu_2O/TiO_2$ exhibited the lowest PL intensity and most efficient separation of photogenerated charges, which may potentially contribute to enhanced photocatalytic activity of $Pt\text{-}Cu_2O/TiO_2$.

3.2. CO_2 photocatalytic reduction

Fig. 6 and Table 2 show the yields and product selectivity of H_2, CO, and CH_4 using different catalysts. The amounts of H_2, CH_4, and CO all increased almost linearly with the reaction time, suggesting that the generation of H_2, CH_4, and H_2 over our catalysts proceeded in a steady-state manner but not a transient manner [18]. Comparing to pristine TiO_2, Pt/TiO_2 significantly enhanced the production of H_2 and CH_4 while inhibited that of CO, which can be attributed to reduced electron-hole recombination (in good accordance with the PL spectra). Differing from Pt, Cu_2O promoted the production of CH_4 but suppressed that of H_2. Moreover, the CH_4 yield of Cu_2O/TiO_2 was lower than that of Pt/TiO_2. This can be explained by the higher electron–hole recombination rate in Cu_2O/TiO_2, which was confirmed by comparing different PL spectra. Moreover, it seems that Pt preferred to activate H_2O while Cu_2O intended to reduce CO_2, which was similar to the results from reported literatures [19,30]. For $Pt\text{-}Cu_2O/TiO_2$ catalyst, the productions of H_2 and CO were both effectively inhibited and CO_2 was selectively converted into CH_4 (selectivity = 96.6%), which may be attributed to the co-deposition of Pt and Cu_2O cocatalysts. The product selectivity of different catalyst will be discussed later in detail.

The O_2 yields during the photocatalytic reaction were also measured (Table 2). On one hand, for $Pt\text{-}Cu_2O/TiO_2$, the O_2 yield was 2.95 μmol g^{-1} h^{-1}. On the other hand, we also estimated the stoichiometric yield of O_2 from the product yields of H_2, CH_4 and CO.

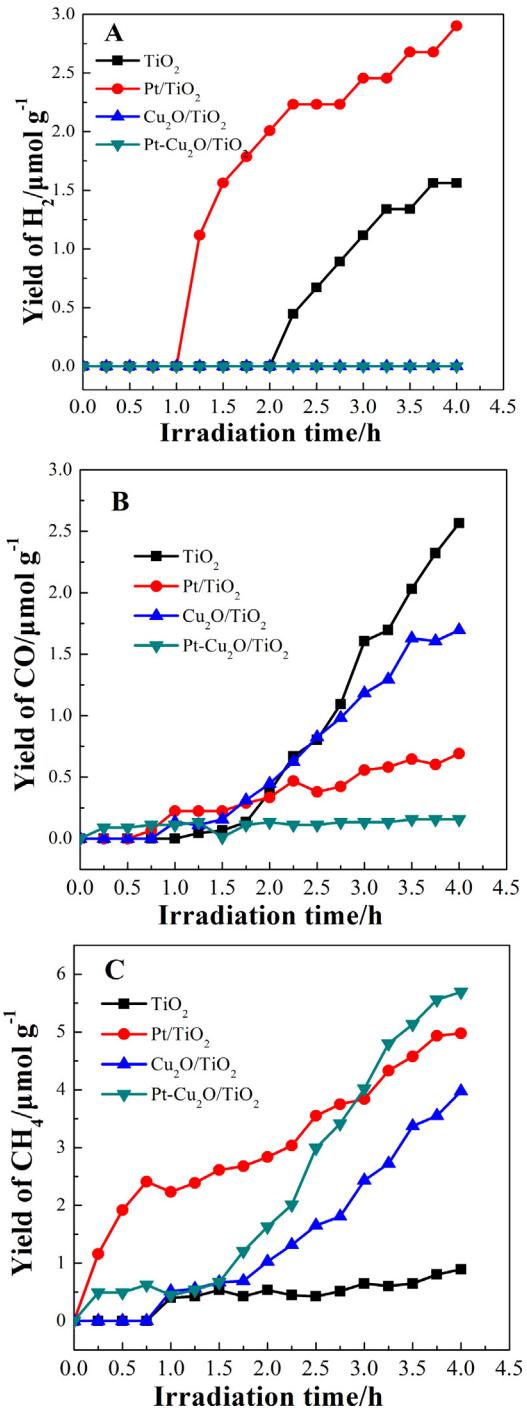

Fig. 6. H_2 (A), CO (B), and CH_4 (C) yields over the catalysts.

The calculation shows as follows: stoichiometric yield of O_2 = (H_2 yield)/2 + (CH_4 yield) × 8 + (CO yield)/2 = 2.87 μmol g^{-1} h^{-1}, which was only slightly lower than the average production rate of O_2, indicating that H_2, CH_4 and CO were the main products of $Pt\text{-}Cu_2O/TiO_2$.

Fig. 7 shows the cycle performance of $Pt\text{-}Cu_2O/TiO_2$ catalyst. After the first cycle, the used $Pt\text{-}Cu_2O/TiO_2$ catalyst was collected and the same experimental process was repeated. The yields of CH_4 and CO in the second and the third cycle were similar to those in the first cycle. This suggests that the reactions over the $Pt\text{-}Cu_2O/TiO_2$ catalyst are catalytic reactions but not stoichiometric ones [18]. Besides, the results in Fig. 7 also indicate that the cycle performance of $Pt\text{-}Cu_2O/TiO_2$ catalyst is good under our reaction conditions.

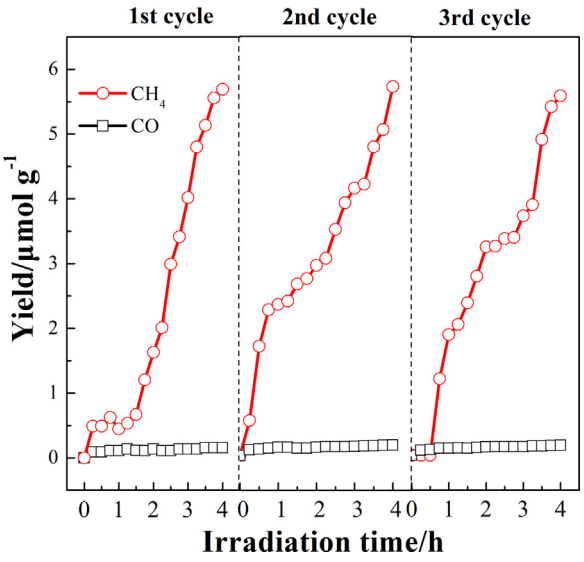

Fig. 7. Cycle photocatalytic performance of Pt-Cu_2O/TiO_2 catalyst.

3.3. Determination of the active sites for CO_2 reduction

Generally, Pt serves as active site for water reduction while Cu_2O is responsible for CO_2 reduction [19,30]. Considering the possible transformation of the cocatalysts, especially Cu species, during the photocatalytic reaction, XPS spectra of the catalysts after photocatalytic reaction were also recorded and compared with those before the reaction (Fig. 8). As shown in Fig. 8A, the binding energy of Pt 4f peaks in Pt/TiO_2 catalyst remained unchanged after reaction, indicating the chemical state of Pt in Pt/TiO_2 was stable during the reaction. Combining the photocatalytic activity of Pt/TiO_2, Pt in Pt/TiO_2 works as the active site for the reduction of CO_2 and water. For Cu_2O/TiO_2 catalyst, the Cu existed in Cu_2O form before reaction (Fig. 8B). After 4 h reaction, Cu_2O was partially reduced into elemental Cu. This can be explained by the reduction of Cu_2O by trapped photogenerated electrons. For Pt-Cu_2O/TiO_2 catalyst (Fig. 8C–D), most of Cu_2O were reduced to elemental Cu after reaction, indicating that the deposition of Pt promoted the electron transfer to Cu_2O during photocatalytic reaction.

Considering the good stability of Pt-Cu_2O/TiO_2 catalysts even after most of Cu_2O was reduced to Cu, it is necessary to investigate the effect of Cu on CO_2 photocatalytic reduction. Cu (0) deposited TiO_2 (Cu/TiO_2) was prepared by the reduction of Cu_2O/TiO_2 under a flow of 5% H_2/N_2 at 250 °C for 3 h. Similarly, Pt and Cu (0) co-deposited TiO_2 catalyst (Pt-Cu/TiO_2) was by the reduction of Pt-Cu_2O/TiO_2. The XPS spectra in Fig. S1 in the online version at DOI: http://dx.doi.org/10.1016/j.apcatb.2016.10.001 indicated that the Cu_2O NPs in Cu_2O/TiO_2 and Pt-Cu_2O/TiO_2 were both totally reduced to Cu after H_2 reduction, while the chemical state of Pt had no significant change. Fig. 9A shows the photocatalytic activities of Cu/TiO_2 and Cu_2O/TiO_2. The results show that Cu loading also enhances the CH_4 production of TiO_2. This is because Cu(0) can also capture photogenerated electrons and work as the active site

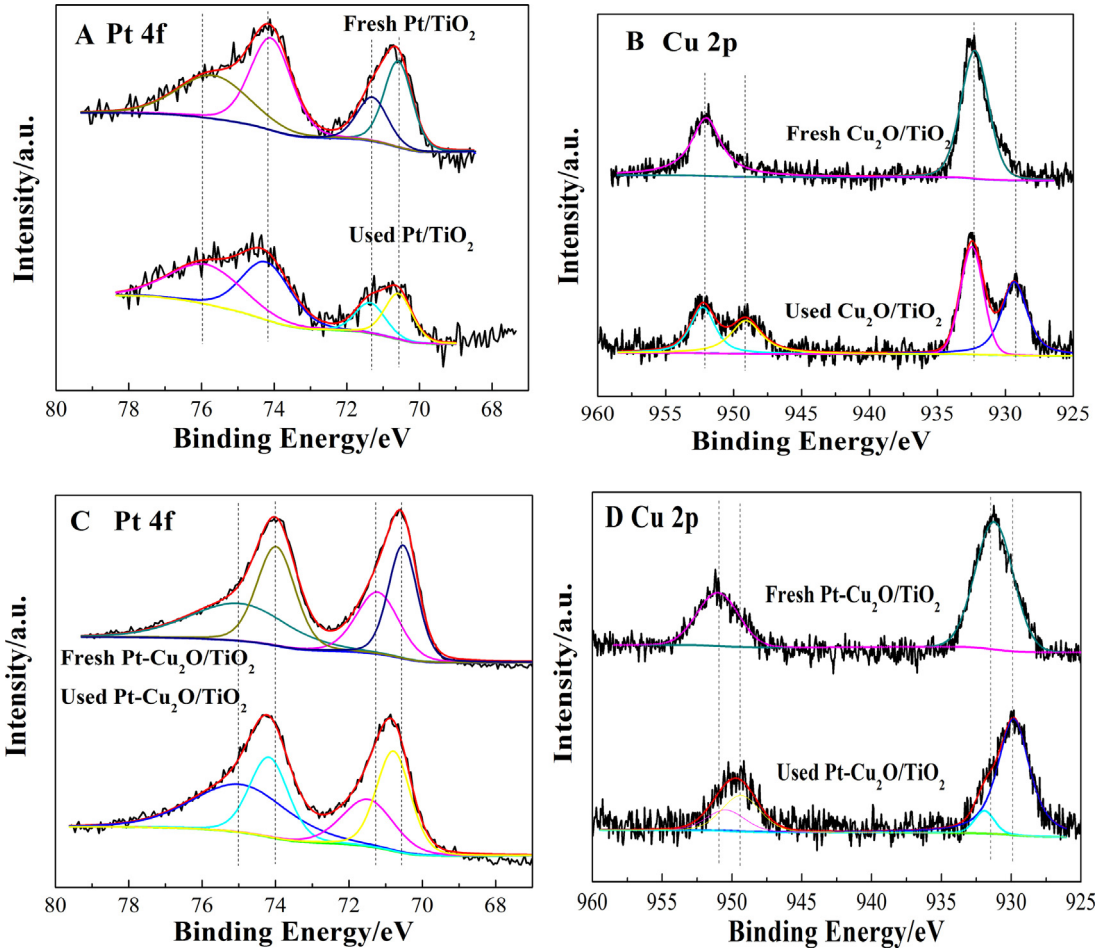

Fig. 8. XPS spectra of the catalyst before and after photocatalytic reaction: (A) Pt 4f spectra of Pt/TiO_2; (B) Cu 2p spectra of Cu_2O/TiO_2; (C) Pt 4f spectra of Pt-Cu_2O/TiO_2; (D) Cu 2p spectra of Pt-Cu_2O/TiO_2.

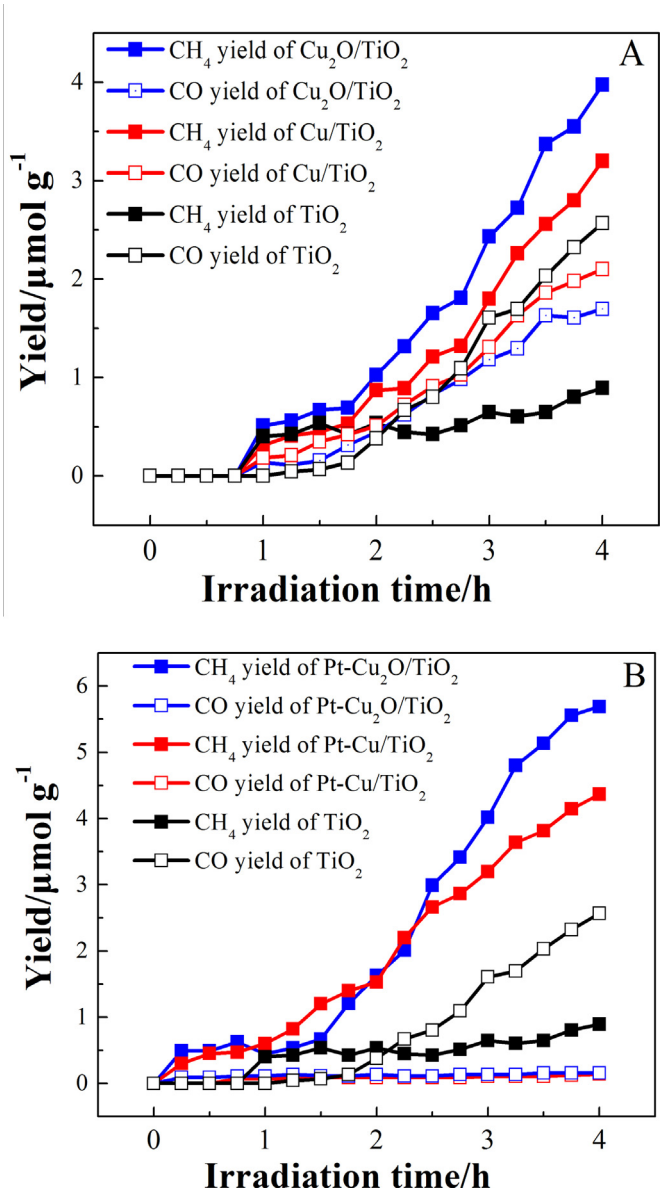

Fig. 9. Photocatalytic activity of Cu/TiO_2 (A)and Pt-Cu/TiO_2 (B) catalysts.

for CO_2 reduction [9]. The higher activity of Cu_2O/TiO_2 indicated Cu_2O is a more effective active site than Cu. Similarly, as shown in Fig. 9B, Pt-Cu/TiO_2 also exhibited high CH_4 production although it is slightly lower than that of Pt-Cu_2O/TiO_2. This can explain the good cycle performance of Pt-Cu_2O/TiO_2. That is although most of the Cu_2O in Pt-Cu_2O/TiO_2 was reduced to Cu after photocatalytic reaction, Cu still trapped photogenerated electrons and served as the active site for CO_2 reduction. In addition, the partial reduction of Cu_2O to Cu would lead to the formation of Cu_2O—Cu/TiO_2 structure, which can prolong the lifetime of the electrons [26], enhancing the efficiency of CO_2 photocatalytic reduction.

3.4. Discussion on the reaction mechanism

The mechanism plays a decisive part in both the selectivity of photo-excited electrons for CO_2 reduction and that of products of CO_2 reduction. The present work has demonstrated that deposition of both Pt and Cu_2O NPs significantly enhanced the selectivity of photogenerated electrons for CO_2 and the production of CH_4.

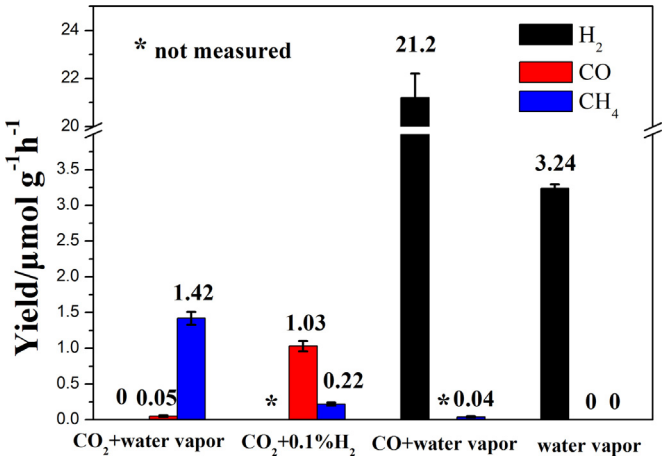

Fig. 10. The catalytic behavior of Pt-Cu_2O/TiO_2 catalyst in the control experiments.

Table 3
The catalytic performance of Pt-Cu_2O/TiO_2 catalyst in control experiments[a].

Reaction atmosphere	Yield/μmol g^{-1} h^{-1}		
	H_2	CO	CH_4
CO_2 + water vapor	0	0.05	1.42
CO_2+ H_2[b]	–	1.03	0.22
CO + water vapor	21.2	–	0.04
Water vapor	3.24	0	0

[a] Reaction conditions: catalyst, 0.020 g; CO_2 pressure, 71 kPa; H_2O, 5 mL; irradiation time, 4 h.
[b] The molar ratio of H_2 to CO_2 is 0.1%.

3.4.1. The high selectivity of photogenerated electrons for CO_2 reduction

The results in Fig. 6 show that the high selectivity of Pt-Cu_2O/TiO_2 for CO_2 reduction resulted from the deposited Cu_2O, which remarkably inhibited the production of H_2. The Cu_2O may suppress H_2 production through three possible routes. First, the H_2 produced from water splitting may be consumed by the reduction of Cu_2O. Second, H_2 can also be consumed by the hydrogenation of CO_2/CO [26,31]. Third, the interfacial contact between water and catalyst might be inhibited and results in low H_2 production. For example, Zhai et al. [19] found that H_2 production was suppressed when the Pt on TiO_2 was covered by Cu_2O layer. Similarly, Xie et al. [18] reported that MgO loaded Pt/TiO_2 obviously enhanced the CO_2 adsorption on TiO_2 so that the adsorption of water on TiO_2 was inhibited, resulting in low H_2 production.

Considering the low Cu_2O loading content, the reduction of Cu_2O cannot be the key factor for the completely inhibited H_2 production over the catalyst. In order to verify the possibility of the last two cases, we performed several control experiments to investigate the reaction pathway of CO_2 reduction over Pt-Cu_2O/TiO_2 (as shown in Fig. 10 and Table 3). In the case of CO_2 hydrogenation with H_2 addition, the CO and CH_4 yield were much higher and lower than those with water as reductant. This indicated that H_2 reduced CO_2 into CO but was difficult to further reduce CO into CH_4. In the case of CO reduction with water vapor, the H_2 yield was remarkably higher while the CH_4 yield was much lower than those of CO_2 reduction with water vapor. The enhanced H_2 production can be attributed to the water-gas shift (WGS) reaction, namely, $CO + H_2O \rightarrow CO_2 + H_2$ [1]. The reduced CH_4 yield refers to the insufficiency of effective CO reduction into CH_4 by H_2 or water vapor, although CO is believed to be more active. These results demonstrate that the consumption of H_2 by CO_2/CO hydrogenation was not the main cause for low H_2 yield of Pt-Cu_2O/TiO_2 during CO_2 photoreduction. Based on the above-mentioned contents, we propose that CH_4 should

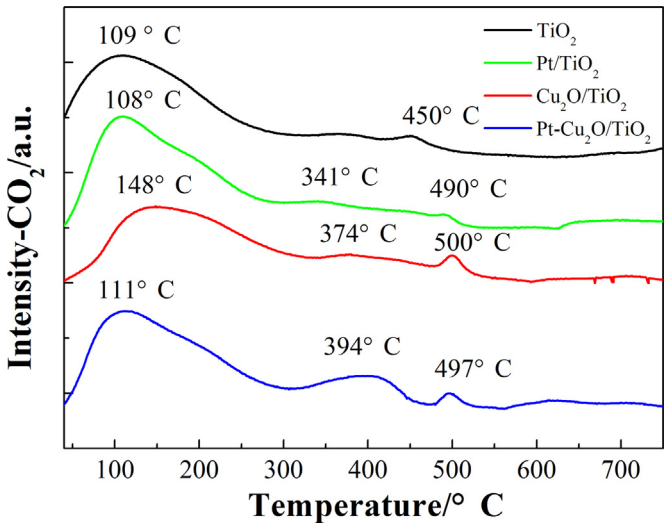

Fig. 11. TPD-CO_2 profiles for the catalysts.

be mainly produced through the direct photocatalytic reduction of CO_2 into CH_4 while a part of CH_4 may come from the photocatalytic reduction of CO.

Moreover, we also tested the H_2 production of Pt-Cu_2O/TiO_2 in the absence of CO_2 (Fig. 8, Table 3). Comparing to the H_2 production of Pt-Cu_2O/TiO_2 in the presence of CO_2, the result clearly shows the existence CO_2 obviously inhibited the production of H_2. Considering the competitive adsorption of CO_2 and H_2O on the surface of TiO_2 [18,19,32], we suppose the low H_2 yield of Pt-Cu_2O/TiO_2 in the presence of CO_2 is mainly caused by the suppressed water adsorption on TiO_2 due to the enhanced CO_2 absorption induced by Cu_2O.

To investigate the effect of Pt and Cu_2O NPs on CO_2 adsorption of the catalyst, TPD-CO_2 of all the samples were performed and the results are shown in Fig. 11. The profiles of TiO_2 show CO_2 desorption at low temperatures, with T_{max} equal to 109 °C and 450 °C, respectively, indicating low interaction between CO_2 and the photocatalyst. This interaction may be slightly higher for Pt/TiO_2 due to the higher desorption temperature at 341 °C and 490 °C. For Cu_2O/TiO_2 and Pt-Cu_2O/TiO_2, their profiles show higher desorption peaks at temperatures of 148, 374, 500 °C and 111, 394, and 497 °C, respectively, indicating Cu_2O cocatalyst can enhanced the interaction between CO_2 and the photocatalyst. The amounts of CO_2 chemisorbed by the catalysts were calculated and summarized in Table 2. The CO_2 chemisorption of TiO_2 was the lowest among all the samples. Besides, the effect of Pt on the CO_2 chemisorption was not obvious, however, the CO_2 chemisorption remarkably enhanced while Cu_2O was deposited on TiO_2. The CO_2 chemisorptions of Cu_2O/TiO_2 and Pt-Cu_2O/TiO_2 were 10.6 and 11.0 μmol g^{-1}, respectively, which are much higher than that of TiO_2 (6.3 μmol g^{-1}) and Pt/TiO_2 (6.8 μmol g^{-1}), indicating an increase in the photocatalyst affinity from Cu_2O deposition. Comparably, Paulino et al. also reported that Cu/TiO_2 obviously enhanced the CO_2 chemisorption of TiO_2 [33]. Combing with the results of control experiments, we confirmed our speculation that the high selectivity of Pt-Cu_2O/TiO_2 for CO_2 reduction was mainly caused by the enhanced CO_2 absorption induced by Cu_2O, which also led to the suppression of water adsorption on TiO_2. However, we still cannot rule out the possibility that part of H_2 was consumed by CO_2/CO hydrogenation and Cu_2O reduction.

3.4.2. The high CH_4 selectivity in CO_2 photoreduction

It has been widely accepted by many researchers that the formation of CH_4 and CO are the compromise between charge transfer and thermodynamics [18,27]. The formation of CH_4 is thermodynamically more feasible than that of CO [34]. That means CH_4 will be selectively formed if enough protons and electrons are supplied. CO was formed as the main product over TiO_2, which possibly results from the low electron density over TiO_2. As mentioned previously, CH_4 was formed through the direct reduction of CO_2. Thus, it is easy to understand that Pt/TiO_2 and Cu_2O/TiO_2 exhibit higher CH_4 selectivity because both Pt and Cu_2O NPs captures photogenerated electrons and increase the electrons density on them as evidenced by the PL spectra, which enhance the probability of multielectron reactions to form CH_4. It is worth noting that the CH_4 selectivity further increased by loading both Pt and Cu_2O onto TiO_2 catalyst. This is because the simultaneous loading of Pt and Cu_2O trap photogenerated electrons and promote the separation of photogenerated electrons and holes more effectively (also proved by PL spectra).

In addition, the Cu 2p XPS spectra of the fresh Cu_2O/TiO_2 and Pt-Cu_2O/TiO_2 catalysts (shown in Fig. 4C–D) have shown that the addition of Pt can enhance the electron density on Cu_2O particles, resulting in higher CH_4 selectivity of Pt-Cu_2O/TiO_2. And the XPS spectra of the used Cu_2O/TiO_2 and Pt-Cu_2O/TiO_2 catalysts (as shown in Fig. 8) demonstrated that the presence of Pt promoted the reduction of Cu_2O during reaction, indicating accelerated electron transfer to Cu_2O during reaction. This contributes to the enough supply of photogenerated electrons for CH_4 production.

Based on the results, it can be concluded that the deposition of Cu_2O enhanced the CO_2 chemisorption on the surface of TiO_2, which accelerated the reduction of CO_2 and suppressed that of H_2O. Meanwhile, the loaded Pt promoted the migration of excited electrons towards the cocatalysts and effectively enhanced the electron density on Cu_2O particles. Consequently, the absorbed CO_2 was sufficiently supplied with photogenerated electrons and selectively reduced to CH_4.

4. Conclusions

Pt and Cu_2O NPs co-depositedTiO$_2$ nanocrystals with co-exposed {001} and {101} facets were prepared through a solvothermal method combining with a $NaBH_4$ reduction method. Pt remarkably promoted the production of H_2 and CH_4 while suppressed the formation of CO. Cu_2O enhanced the generation of CH_4 while suppressed the production of H_2. When Pt and Cu_2O were co-deposited on TiO_2 crystals, the productions of H_2 and CO were both effectively inhibited and CO_2 was selectively converted into CH_4 (selectivity = 96.6%). We demonstrated that CH_4 was mainly produced through the direct photocatalytic reduction of CO_2 into CH_4 rather than the hydrogenation of intermediate products such as CO. The deposition of Cu_2O enhanced the CO_2 chemisorption on TiO_2 and inhibited that of water, resulting in enhanced CO_2 reduction and suppressed H_2 production. The Pt loading captured photogenerated electrons and increased the electrons density on the cocatalysts, which was advantageous to the selective formation of CH_4. The high CH_4 selectivity of Pt-Cu_2O/TiO_2 catalysts can be attributed to the co-loading of Cu_2O and Pt NPs, which enhanced the CO_2 chemisorption and electron density on the surface of TiO_2 simultaneously.

Acknowledgments

This project was supported by the National Key Basic Research and Development Program (2011CB707301), the National Key Technology R&D Program (2011BAC05B00), the Program of International S&T Cooperation (2012DFB60100), the Foundation of State Key Laboratory of Coal Combustion (FSKLCCB1402), and the Foreign Science and Technology Cooperation of Hubei Province. The authors acknowledge the Analysis and Test Center of Huazhong University of Science & Technology.

References

[1] Y.-H. Cheng, V.-H. Nguyen, H.-Y. Chan, J.C.S. Wu, W.-H. Wang, Photo-enhanced hydrogenation of CO_2 to mimic photosynthesis by CO co-feed in a novel twin reactor, Appl. Energy 147 (2015) 318–324.

[2] W. Li, Y. Shi, Y. Luo, Y. Wang, N. Cai, Carbon monoxide/carbon dioxide electrochemical conversion on patterned nickel electrodes operating in fuel cell and electrolysis cell modes, Int. J. Hydrogen Energy 41 (2016) 3762–3773.

[3] W.-H. Lee, C.-H. Liao, M.-F. Tsai, C.-W. Huang, J.C.S. Wu, A novel twin reactor for CO_2 photoreduction to mimic artificial photosynthesis, Appl. Catal. B: Environ. 132–133 (2013) 445–451.

[4] T. Inoue, A. Fujishima, S. Konishi, K. Honda, Photoelectrocatalytic reduction of carbon dioxide in aqueous suspensions of semiconductor powders, Nature 277 (1979) 637–638.

[5] Z. Xiong, Y. Zhao, J. Zhang, C. Zheng, Efficient photocatalytic reduction of CO_2 into liquid products over cerium doped titania nanoparticles synthesized by a sol–gel auto-ignited method, Fuel Process. Technol. 135 (2015) 6–13.

[6] C.-W. Huang, C.-H. Liao, J.C.S. Wu, Y.-C. Liu, C.-L. Chang, C.-H. Wu, M. Anpo, M. Matsuoka, M. Takeuchi, Hydrogen generation from photocatalytic water splitting over TiO2 thin film prepared by electron beam-induced deposition, Int. J. Hydrogen Energy 35 (2010) 12005–12010.

[7] M. Pelaez, N.T. Nolan, S.C. Pillai, M.K. Seery, P. Falaras, A.G. Kontos, P.S.M. Dunlop, J.W.J. Hamilton, J.A. Byrne, K. O'Shea, M.H. Entezari, D.D. Dionysiou, A review on the visible light active titanium dioxide photocatalysts for environmental applications, Appl. Catal. B: Environ. 125 (2012) 331–349.

[8] Y. Li, W.-N. Wang, Z. Zhan, M.-H. Woo, C.-Y. Wu, P. Biswas, Photocatalytic reduction of CO_2 with H_2O on mesoporous silica supported Cu/TiO_2 catalysts, Appl. Catal. B: Environ. 100 (2010) 386–392.

[9] J.Z.Y. Tan, Y. Fernández, D. Liu, M. Maroto-Valer, J. Bian, X. Zhang, Photoreduction of CO_2 using copper-decorated TiO_2 nanorod films with localized surface plasmon behavior, Chem. Phys. Lett. 531 (2012) 149–154.

[10] Y. Wang, B. Li, C. Zhang, L. Cui, S. Kang, X. Li, L. Zhou, Ordered mesoporous CeO_2-TiO_2 composites: highly efficient photocatalysts for the reduction of CO_2 with H_2O under simulated solar irradiation, Appl. Catal. B: Environ. 130–131 (2013) 277–284.

[11] Z. Zhang, B. Dong, M. Zhang, J. Huang, F. Lin, C. Shao, Electrospun Pt/TiO_2 hybrid nanofibers for visible-light-driven H_2 evolution, Int. J. Hydrogen Energy 39 (2014) 19434–19443.

[12] W.N. Wang, W.J. An, B. Ramalingam, S. Mukherjee, D.M. Niedzwiedzki, S. Gangopadhyay, P. Biswas, Size and structure matter: enhanced CO_2 photoreduction efficiency by size-resolved ultrafine Pt nanoparticles on TiO_2 single crystals, J. Am. Chem. Soc. 134 (2012) 11276–11281.

[13] H. Li, X. Wu, J. Wang, Y. Gao, L. Li, K. Shih, Enhanced activity of Ag-MgO-TiO_2 catalyst for photocatalytic conversion of CO_2 and H_2O into CH_4, Int. J. Hydrogen Energy 41 (2016) 8479–8488.

[14] D. Kong, J.Z.Y. Tan, F. Yang, J. Zeng, X. Zhang, Electrodeposited Ag nanoparticles on TiO_2 nanorods for enhanced UV visible light photoreduction CO_2 to CH_4, Appl. Surf. Sci. 277 (2013) 105–110.

[15] H. Xu, S. Ouyang, L. Liu, D. Wang, T. Kako, J. Ye, Porous-structured Cu_2O/TiO_2 nanojunction material toward efficient CO_2 photoreduction, Nanotechnology 25 (2014) 165402.

[16] X. Liu, Y.-y. Hu, R.-Y. Chen, Z. Chen, H.-C. Han, Coaxial nanofibers of ZnO-TiO_2 heterojunction with high photocatalytic activity by electrospinning technique, Synt. React. Inorg. Met.-Org. Nano-Met. Chem. 44 (2013) 449–453.

[17] Z. Xiong, Y. Luo, Y. Zhao, J. Zhang, C. Zheng, J.C. Wu, Synthesis, characterization and enhanced photocatalytic CO_2 reduction activity of graphene supported TiO_2 nanocrystals with coexposed {001} and {101} facets, Phys. Chem. Chem. Phys. 18 (2016) 13186–13195.

[18] S. Xie, Y. Wang, Q. Zhang, W. Deng, Y. Wang, MgO- and Pt-promoted TiO_2 as an efficient photocatalyst for the preferential reduction of carbon dioxide in the presence of water, ACS Catal. 4 (2014) 3644–3653.

[19] Q. Zhai, S. Xie, W. Fan, Q. Zhang, Y. Wang, W. Deng, Y. Wang, Photocatalytic conversion of carbon dioxide with water into methane: platinum and copper(I) oxide co-catalysts with a core-shell structure, Angew. Chem. 52 (2013) 5776–5779.

[20] Z. Xiong, H. Wang, N. Xu, H. Li, B. Fang, Y. Zhao, J. Zhang, C. Zheng, Photocatalytic reduction of CO_2 on Pt^{2+}–Pt^0/TiO_2 nanoparticles under UV/Vis light irradiation: a combination of Pt^{2+} doping and Pt nanoparticles deposition, Int. J. Hydrogen Energy 40 (2015) 10049–10062.

[21] J. Yu, J. Low, W. Xiao, P. Zhou, M. Jaroniec, Enhanced photocatalytic CO_2-reduction activity of anatase TiO_2 by coexposed {001} and {101} facets, J. Am. Chem. Soc. 136 (2014) 8839–8842.

[22] Z. Zhang, Z. Wang, S.-W. Cao, C. Xue, Au/Pt nanoparticle-decorated TiO_2 nanofibers with plasmon-enhanced photocatalytic activities for solar-to-fuel conversion, J. Phys. Chem. C 117 (2013) 25939–25947.

[23] L. Zhang, R.V. Koka, A study on the oxidation and carbon diffusion of TiC in alumina?titanium carbide ceramics using XPS and Raman spectroscopy, Mater. Chem. Phys. 57 (1998) 23–32.

[24] B. Fang, N.K. Chaudhari, M.-S. Kim, J.H. Kim, J.-S. Yu, Homogeneous deposition of platinum nanoparticles on carbon black for proton exchange membrane fuel cell, J. Am. Chem. Soc. 131 (2009) 15330–15338.

[25] S. Lee, S. Jeong, W.D. Kim, S. Lee, K. Lee, W.K. Bae, J.H. Moon, S. Lee, D.C. Lee, Low-coordinated surface atoms of CuPt alloy cocatalysts on TiO_2 for enhanced photocatalytic conversion of fx1fx2CO_2, Nanoscale 8 (2016) 10043–10048.

[26] B.R. Chen, V.H. Nguyen, J.C. Wu, R. Martin, K. Koci, Production of renewable fuels by the photohydrogenation of CO_2: effect of the Cu species loaded onto TiO_2 fx7photocatalysts, Phys. Chem. Chem. Phys. 18 (2016) 4942–4951.

[27] W.N. Wang, W.J. An, B. Ramalingam, S. Mukherjee, D.M. Niedzwiedzki, S. Gangopadhyay, P. Biswas, Size and structure matter: enhanced CO_2 photoreduction efficiency by size-resolved ultrafine Pt nanoparticles on TiO_2 single crystals, J. Am. Chem. Soc. 134 (2012) 11276–11281.

[28] J. Wu, Q. Liu, P. Gao, Z. Zhu, Influence of praseodymium and nitrogen co-doping on the photocatalytic activity of TiO_2, Mater. Res. Bull. 46 (2011) 1997–2003.

[29] C. Liu, X. Han, S. Xie, Q. Kuang, X. Wang, M. Jin, Z. Xie, L. Zheng, Enhancing the photocatalytic activity of anatase TiO_2 by improving the specific facet-induced spontaneous separation of photogenerated electrons and holes, Chem.: Asian J. 8 (2013) 282–289.

[30] O.K. Varghese, M. Paulose, T. LaTempa, C.A. Grimes, High-rate solar photocatalytic conversion of CO_2 and water vapor to hydrocarbon fuels, Nano Lett. 9 (2008) 731–737.

[31] G. Guan, T. Kida, A. Yoshida, Reduction of carbon dioxide with water under concentrated sunlight using photocatalyst combined with Fe-based catalyst, Appl. Catal. B: Environ. 41 (2003) 387–396.

[32] J.C.S. Wu, H.-M. Lin, C.-L. Lai, Photo reduction of CO_2 to methanol using optical-fiber photoreactor, Appl. Catal. A: Gen. 296 (2005) 194–200.

[33] P.N. Paulino, V.M.M. Salim, N.S. Resende, Zn-Cu promoted TiO_2 photocatalyst for CO_2 reduction with H_2O under UV light, Appl. Catal. B: Environ. 185 (2016) 362–370.

[34] A.J. Morris, G.J. Meyer, E. Fujita, Molecular approaches to the photocatalytic reduction of carbon dioxide for solar fuels, Acc. Chem. Res. 42 (2009) 1983–1994.